Important Notice to Authors

Attached is a PDF proof of your forthcoming article in PRE. Your article has 8 pages and the Accession Code is **LG15153E**.

Please note that as part of the production process, APS converts all articles, regardless of their original source, into standardized XML that in turn is used to create the PDF and online versions of the article as well as to populate third-party systems such as Portico, CrossRef, and Web of Science. We share our authors' high expectations for the fidelity of the conversion into XML and for the accuracy and appearance of the final, formatted PDF. This process works exceptionally well for the vast majority of articles; however, please check carefully all key elements of your PDF proof, particularly any equations or tables.

Figures submitted electronically as separate PostScript files containing color usually appear in color in the online journal. However, all figures will appear as grayscale images in the print journal unless the color figure charges have been paid in advance, in accordance with our policy for color in print (http://publish.aps.org/authors/color-figures-print) and the relevant figure captions read "Color". For figures that will be color online but grayscale in print, please ensure that the text and captions clearly describe the figures to readers who view the article only in grayscale.

No further publication processing will occur until we receive your response to this proof.

Specific Questions and Comments to Address for This Paper

INSTRUCTIONS TO AUTHOR: Please make sure that color online figures can also be understood in the printed black-and-white version. Modify figures and/or captions if needed.

1 Please check that authors correspond with their correct affiliations.

2 Would changing "sgn(I)" and "abs(I)" to "sign of I" and "absolute value of I" respectively in the abstract only be more clear?

3 Please remove duplicate entry (i.e., Refs. 5 and 7) from the reference list and renumber all subsequent reference citations in both the text and in the reference list.

4 Please check author initials in Ref. 24.

Q: This reference could not be uniquely identified due to incomplete information or improper format. Please check all information and amend if applicable.

Other Items to Check

- Please note that the original manuscript has been converted to XML prior to the creation of the PDF proof, as described above. Please carefully check all key elements of the paper, particularly the equations and tabular data.
- Please check PACS numbers. More information on PACS numbers is available online at http://publish.aps.org/PACS/.
- Title: Please check; be mindful that the title may have been changed during the peer review process.
- Author list: Please make sure all authors are presented, in the appropriate order, and that all names are spelled correctly.
- Please make sure you have inserted a byline footnote containing the email address for the corresponding author, if desired. Please note that this is not inserted automatically by this journal.
- Affiliations: Please check to be sure the institution names are spelled correctly and attributed to the appropriate author(s).
- Receipt date: Please confirm accuracy.
- Acknowledgments: Please be sure to appropriately acknowledge all funding sources.
- Hyphenation: Please note hyphens may have been inserted in word pairs that function as adjectives when they occur before a noun, as in "x-ray diffraction," "4-mm-long gas cell," and "*R*-matrix theory." However, hyphens are deleted from word pairs when they are not used as adjectives before nouns, as in "emission by x rays," "was 4 mm in length," and "the *R* matrix is tested."

  Note also that Physical Review follows U.S. English guidelines in that hyphens are not used after prefixes or before suffixes: superresolution, quasiequilibrium, nanoprecipitates, resonancelike, clockwise.
- Please check that your figures are accurate and sized properly. Make sure all labeling is sufficiently legible. Figure quality in this proof is representative of the quality to be used in the online journal. To achieve manageable file size for online delivery, some compression and downsampling of figures may have occurred. Fine details may have become somewhat fuzzy, especially in color figures. The print journal uses files of higher resolution and therefore details may be sharper in print. Figures to be published in color online will appear in color on these proofs if viewed on a color monitor or printed on a color printer.
- ***Overall, please proofread the entire article very carefully.***

Ways to Respond

- ***Web:*** If you accessed this proof online, follow the instructions on the web page to submit corrections.

- ***Email:*** Send corrections to preproofs@aptaracorp.com
  Subject: **LG15153E** proof corrections
- ***Fax:*** Return this proof with corrections to +1.703.791.1217. Write **Attention:** PRE Project Manager and the Article ID, **LG15153E**, on the proof copy unless it is already printed on your proof printout.
- ***Mail:*** Return this proof with corrections to **Attention:** PRE Project Manager, Physical Review E, c/o Aptara, 3110 Fairview Park Drive, Suite #900, Falls Church, VA 22042-4534, USA.

PHYSICAL REVIEW E **00**, 002100 (2013)

Nonequilibrium steady state and induced currents of a mesoscopically glassy system: Interplay of resistor-network theory and Sinai physics

Daniel Hurowitz,[1] Saar Rahav,[2] and Doron Cohen[1]
[1]*Department of Physics, Ben-Gurion University of the Negev, Beer-Sheva, Israel*
[2]*Schulich Faculty of Chemistry, Technion–Israel Institute of Technology, Haifa 32000, Israel*

(Received 25 July 2013; revised manuscript received 22 September 2013; published xxxxxx)

We introduce an explicit solution for the nonequilibrium steady state (NESS) of a ring that is coupled to a thermal bath, and is driven by an external hot source with log-wide distribution of couplings. Having time scales that stretch over several decades is similar to glassy systems. Consequently there is a wide range of driving intensities where the NESS is like that of a random walker in a biased Brownian landscape. We investigate the resulting statistics of the induced current I. For a single ring we discuss how $\mathrm{sgn}(I)$ fluctuates as the intensity of the driving is increased, while for an ensemble of rings we highlight the fingerprints of Sinai physics on the $\mathrm{abs}(I)$ distribution.

DOI: 10.1103/PhysRevE.00.002100 PACS number(s): 05.70.Ln, 05.60.−k, 05.40.−a, 73.23.−b

I. INTRODUCTION

The transport in a chain due to random nonsymmetric transition probabilities is a fundamental problem in statistical mechanics [1–7]. This type of dynamics is of great relevance for surface diffusion [8] and thermal ratchets [9–12] and was used to model diverse biological systems, such as molecular motors, enzymes, and unidirectional motion of proteins along filaments [13–16]. Of particular interest are applications that concern the conduction of DNA segments [17,18], and thin glassy electrolytes under high voltages [19–23].

Mathematically one can visualize the dynamics as *a random walk in a random environment*: a particle that makes incoherent jumps between "sites" of a network. In an unbounded quasi-one-dimensional network we might have either diffusion or subdiffusive Sinai spreading [6], depending on whether the transition rates form a symmetric matrix or not. In contrast, when the system is bounded (and without disjoint components) it eventually reaches a well-defined steady state. This would be an equilibrium *canonical* (Boltzmann) state if the transition rates were detailed balanced, else it is termed nonequilibrium steady state (NESS).

Considering the NESS of a mesoscopically glassy system, *our working hypothesis is that glassiness might lead to a novel NESS with fingerprints of Sinai physics*. By "glassiness" we mean that the rates that are induced by a bath, or by an external source, have a log-wide distribution, hence many time scales are involved [24] as in spin-glass models [25]. Having a log-wide distribution of time scales is typical for hopping in a random energy landscape, where the rates depend exponentially on the barrier heights. It also arises in driven quasi-integrable systems, where due to approximate selection rules there is a "sparse" fraction of large coupling elements, while the majority become very small [26].

The emergence of Sinai physics in a system that is described by a rate equation with asymmetric transition probabilities is not self-evident [27]. An experimental observation of Sinai diffusion regarding the unzipping transition of DNA molecules has been reported [28], and other applications have been considered [29,30]. The nonlinear current dependence of a mesoscopic ring has been theoretically studied in the past [19,23], with references to experiments [20–22], *but the statistical aspects, and the possible relevance of Sinai physics, have not been considered*. In previous publications, we have pointed out that due to "glassiness" Sinai physics becomes a relevant ingredient in the analysis of energy absorption [31] and transport [32] in such a ring system.

In this work we consider a geometrically closed mesoscopic system that has a nontrivial topology. The system is immersed in a finite temperature "cold" bath. Additionally it is coupled to a driving source, with couplings that are log-wide distributed. The driving source can be regarded as a "hot bath" of infinite temperature. Consequently detailed balance is spoiled, and after a transient a NESS is reached. Specifically we consider the simplest possible model: a mesoscopic ring that is made up of N sites. See Fig. 1 for a graphical illustration. Due to the lack of detailed balance a circulating current is induced. We shall see that the value of the current (I) depends in a nonlinear way on the intensity (ν) of the driving source. Our interest is in the statistical aspects of this dependence.

Our model is physically motivated and significantly differs from the standard setup that has been assumed in past literature. Previous study of Sinai-type disordered systems [7] has considered an open geometry with uncorrelated transition rates that have the same coupling everywhere. Consequentially the random-resistor-network aspect (which is related to local variation of the couplings) has not emerged. Furthermore, in the physically motivated setup that we have defined above (ring + bath + driving) Sinai physics would not arise if the couplings to the driving source were merely disorderly random. The log-wide distribution is a crucial ingredient. Finally, in a closed (ring) geometry, unlike an open (two terminal) geometry, the statistics of I is not only affected by the distribution of transition rates, but also by the spatial profile of the NESS. This is like a "canonical" as opposed to a "grand canonical" setting, leading to remarkably different results.

Outline. In Sec. II we describe our minimal model: a ring coupled to a heat bath and to a driving field, with log-wide distribution of coupling. In Sec. III we estimate the number of sign changes of the steady state current $I(\nu)$ as the intensity of the driving is increased. In Secs. IV and V we present an explicit formula for the NESS. This formula is employed in Sec. VI to study the statistical properties of $I(\nu)$ for an

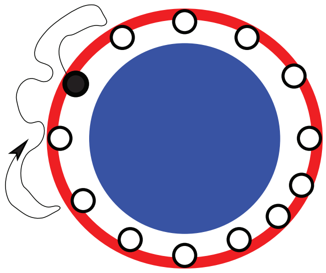

FIG. 1. (Color online) Schematic illustration of the model system. A ring made up of N sites is immersed in a "cold" bath (represented by inner blue circle) and subjected to a "hot" driving source (represented by an outer red circle). The latter has an intensity ν that can be easily controlled experimentally. The transitions rates between the sites of the ring are given by Eq. (1). The dynamics can be optionally regarded as that of a random walker in a random environment. After a transient a NESS is reached with current $I(\nu)$.

ensemble of rings. Specifically, the statistics outside of the Sinai regime is investigated in Sec. VII, while the statistics in the Sinai regime is studied in Sec. VIII. In the latter case we show how the fingerprints of Sinai physics can be extracted from the analysis of $I(\nu)$ curves. The results are summarized in Sec. IX.

II. THE MODEL

Consider a ring that consists of sites labeled by n with positions $x = n$ that are defined modulo N. The bonds are labeled as $\overrightarrow{n} \equiv (n{-}1 \rightsquigarrow n)$. The inverse bond is $\overleftarrow{n}$, and if direction does not matter we label both by $\bar{n}$. The position of the nth bond is defined as $x_n \equiv n{-}(1/2)$. The on-site energies E_n are normally distributed over a range Δ, and the transition rates are between nearest-neighboring sites:

$$w_{\overrightarrow{n}} = w^{\beta}_{\overrightarrow{n}} + \nu g_{\bar{n}}. \tag{1}$$

Here w^{β} are the rates that are induced by a bath that has a finite temperature T_B. The $g_{\bar{n}}$ are couplings to a driving source that has an intensity ν. These couplings are log-box distributed within $[g_{\min}, g_{\max}]$. This means that $\ln(g_{\bar{n}})$ are distributed uniformly over a range $\sigma = \ln(g_{\max}/g_{\min})$. The bath transition rates satisfy detailed balance, namely,

$$\frac{w^{\beta}_{\overrightarrow{n}}}{w^{\beta}_{\overleftarrow{n}}} = \exp\left[-\frac{E_n - E_{n-1}}{T_B}\right]. \tag{2}$$

Assuming $\Delta \ll T_B$ one obtains the following approximation:

$$w^{\beta}_{\overrightarrow{n}} \approx \left[1 - \frac{1}{2}\left(\frac{E_n - E_{n-1}}{T_B}\right)\right] \bar{w}^{\beta}_{\bar{n}}, \tag{3}$$

$$w^{\beta}_{\overleftarrow{n}} \approx \left[1 + \frac{1}{2}\left(\frac{E_n - E_{n-1}}{T_B}\right)\right] \bar{w}^{\beta}_{\bar{n}}. \tag{4}$$

The driving spoils the detailed balance. We define the resulted stochastic field as follows:

$$\mathcal{E}(x_n) \equiv \ln\left[\frac{w_{\overrightarrow{n}}}{w_{\overleftarrow{n}}}\right]. \tag{5}$$

Assuming $\Delta \ll T_B$ we get the following approximation:

$$\frac{w_{\overrightarrow{n}}}{w_{\overleftarrow{n}}} = \frac{w^{\beta}_{\overrightarrow{n}} + \nu g_{\bar{n}}}{w^{\beta}_{\overleftarrow{n}} + \nu g_{\bar{n}}} \approx 1 - \frac{(E_n - E_{n-1})/T_B}{1 + (g_{\bar{n}}/\bar{w}^{\beta}_{\bar{n}})\nu} \tag{6}$$

leading to

$$\mathcal{E}(x_n) \approx -\left[\frac{1}{1 + g_{\bar{n}}\nu}\right] \frac{E_n - E_{n-1}}{T_B}. \tag{7}$$

In the last equality, without loss of generality, the $g_{\bar{n}}$ have been rescaled such that all the bath-induced transitions have the same average value $\bar{w}^{\beta} = 1$.

III. CURRENT SIGN REVERSALS IN THE SINAI REGIME

The direction of the current $\text{sgn}(I)$ is determined by the stochastic motive force (SMF), also known as the affinity, or as the entropy production [33–36]:

$$\mathcal{E}_{\circlearrowleft} \equiv \ln\left[\frac{\prod_n w_{\overrightarrow{n}}}{\prod_n w_{\overleftarrow{n}}}\right] = \oint \mathcal{E}(x)dx. \tag{8}$$

In the second equality we formally regard x as a continuous variable. This will make the later mathematics more transparent. Assuming $\Delta \ll T_B$ we get the following approximation:

$$\mathcal{E}_{\circlearrowleft} \approx -\sum_{n=1}^{N}\left[\frac{1}{1 + g_{\bar{n}}\nu}\right]\frac{\Delta_n}{T_B}. \tag{9}$$

One observes that for $\nu \ll g_{\max}^{-1}$ the SMF is linear, $\mathcal{E}_{\circlearrowleft} \propto \nu$, while for $\nu \gg g_{\min}^{-1}$ it vanishes, $\mathcal{E}_{\circlearrowleft} \propto 1/\nu$. In the intermediate regime, which we call below *the Sinai regime*, the SMF changes sign several times (see Fig. 2). Using the notations

$$\tau \equiv \frac{1}{\sigma}\ln(g_{\max}\nu) \tag{10}$$

and $\tau_n = (1/\sigma)\ln(g_{\max}/g_{\bar{n}})$, the expression for the SMF takes the following form:

$$\mathcal{E}_{\circlearrowleft}(\tau) = -\sum_{n=1}^{N} f_{\sigma}(\tau - \tau_n)\frac{E_n - E_{n-1}}{T_B}, \tag{11}$$

where $f_{\sigma}(t) \equiv [1 + e^{\sigma t}]^{-1}$ drops monotonically from unity to zero like a smoothed step function. If $f(t)$ were a sharp step function it would follow that in the Sinai regime $\mathcal{E}_{\circlearrowleft}(\tau)$ is formally like a random walk [37–39]. The number of sign reversals equals the number of times the random walker crosses the origin. We have here a coarse-grained random walk: The τ_n are distributed uniformly over a range $[0,1]$, and each step is smoothed by $f_{\sigma}(t)$ such that the effective number of coarse-grained steps is σ. Hence we expect the number of sign changes to be not $\sim\sqrt{\pi N}$ but $\sim\sqrt{\pi\sigma}$, reflecting the log-width of the distribution.

IV. ADDING BONDS IN SERIES

The NESS equations are quite simple and can be solved using elementary algebra as in [19,20,23,32], or optionally using the network formalism for stochastic systems [40–42]. Below we propose a generalized resistor-network approach that allows one to obtain a more illuminating version for the NESS, which will provide better insight for the statistical

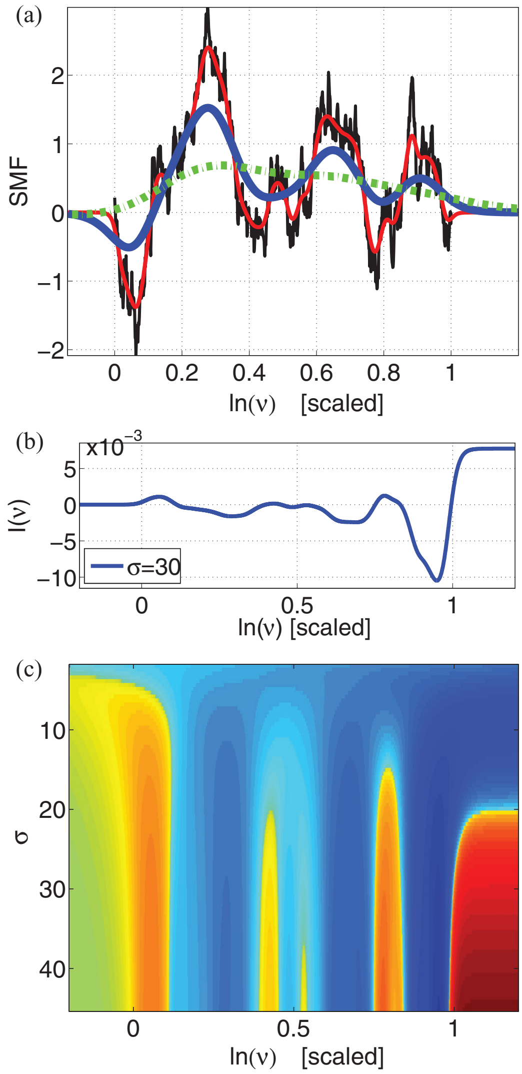

FIG. 2. (Color online) We consider a ring with $N = 1000$ sites whose energies are normally distributed with dispersion $\Delta = 1$. The bath temperature is $T_B = 10$. In (a) the SMF of Eq. (11) is plotted for $\sigma = \infty$, and for $\sigma = 50, 10, 4$. The smaller σ, the smoother ν dependence. In (b) a representative $I(\nu)$ curve is plotted. In (c) a set of $I(\nu)$ curves is color imaged: Each row is $I(\nu)$ for a different σ; blue and red are for positive and negative (clockwise) circulating current, respectively. In all panels the horizontal axis is the scaled driving intensity as defined in Eq. (10).

analysis. Let us assume that we have a NESS with a current I. The steady state equations for two adjacent bonds are

$$I = w_{\overrightarrow{1}} p_0 - w_{\overleftarrow{1}} p_1, \tag{12}$$

$$I = w_{\overrightarrow{2}} p_1 - w_{\overleftarrow{2}} p_2. \tag{13}$$

We can combine them into one equation:

$$I = \overrightarrow{G} p_0 - \overleftarrow{G} p_2, \tag{14}$$

with

$$\overrightarrow{G} \equiv \left[\frac{1}{w_{\overrightarrow{1}}} + \frac{1}{w_{\overrightarrow{2}}}\left(\frac{w_{\overleftarrow{1}}}{w_{\overrightarrow{1}}}\right)\right]^{-1}, \tag{15}$$

$$\overleftarrow{G} \equiv \left[\frac{1}{w_{\overleftarrow{2}}} + \frac{1}{w_{\overleftarrow{1}}}\left(\frac{w_{\overrightarrow{2}}}{w_{\overleftarrow{2}}}\right)\right]^{-1}. \tag{16}$$

We can repeat this procedure iteratively. If we have N bonds in series we get

$$\overrightarrow{G} = \left[\sum_{m=1}^{N} \frac{1}{w_{\overrightarrow{m}}} \exp\left(-\int_0^{m-1} \mathcal{E}(x)dx\right)\right]^{-1}, \tag{17}$$

$$\overleftarrow{G} = \left[\sum_{m=1}^{N} \frac{1}{w_{\overleftarrow{m}}} \exp\left(\int_m^{N} \mathcal{E}(x)dx\right)\right]^{-1}. \tag{18}$$

Coming back to the ring, we can cut it at an arbitrary site n, and calculate the associated G's. It follows that $I = (\overrightarrow{G}_n - \overleftarrow{G}_n)\, p_n$. Consequently the NESS is

$$p_n = \frac{I}{\overrightarrow{G}_n - \overleftarrow{G}_n} \tag{19}$$

and I can be regarded as the normalization factor:

$$I = \left[\sum_{n=1}^{N} \frac{1}{\overrightarrow{G}_n - \overleftarrow{G}_n}\right]^{-1}. \tag{20}$$

In the next paragraph we show how to write these results in an explicit way that illuminates the relevant physics.

V. THE NESS FORMULA

One should notice that Eqs. (17) and (18) cannot be treated on equal footing due to a missmatch between m and $m{-}1$. For this reason we introduced an improved convention for the description of the bonds. We define the conductance of a bond as the geometric mean of the clockwise and anticlockwise transition rates:

$$w(x_n) = \sqrt{w_{\overrightarrow{n}}\, w_{\overleftarrow{n}}}. \tag{21}$$

Hence $w_{\overrightarrow{n}} = w(x_n)\exp[(1/2)\mathcal{E}(x_n)]$. Accordingly Eqs. (17) and (18) can be unified and written as

$$\overrightarrow{G}_n = \left[\sum_{m=n+1}^{N+n} \frac{1}{w(x_m)} \exp\left(-\int_n^{x_m} \mathcal{E}(x)dx\right)\right]^{-1}, \tag{22}$$

with the implicit understanding that the summation and the integration are anticlockwise modulo N. With the new notations it is easy to see that $\overleftarrow{G}_n = \exp(-\mathcal{E}_{\circlearrowleft})\,\overrightarrow{G}_n$. We use the notation G_n for the geometric mean. Consequently the formula for the current takes the form

$$I = \left[\sum_{n=1}^{N} \frac{1}{G_n}\right]^{-1} 2\sinh\left(\frac{\mathcal{E}_{\circlearrowleft}}{2}\right), \tag{23}$$

while $p_n \propto 1/G_n$. Our next task is to find a tractable expression for the latter. Regarding x as an extended coordinate,

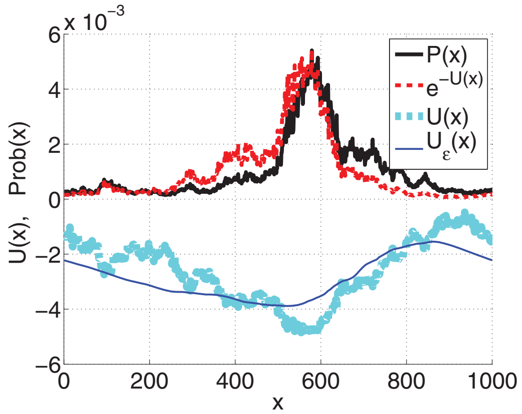

FIG. 3. (Color online) The NESS profile of Eq. (26) (solid black) is similar but not identical to the quasiequilibrium distribution (dashed red line). Also shown (lower curves) is the potential landscape $U(x)$ and its smoothed version $U_\varepsilon(x)$. The parameters are the same as in Fig. 2, with $\sigma = 10$, and driving intensity that corresponds to $\tau = 0.3$. The bonds were rearranged to have a larger SMF, namely, $\mathcal{E}_\circlearrowleft = 7.4$.

the potential $V(x)$ that is associated with the field $\mathcal{E}(x)$ is a tilted periodic potential. Adding $[\mathcal{E}_\circlearrowleft/N]x$ we get a periodic potential $U(x)$ (see Fig. 3). Accordingly

$$\int_{x'}^{x''} \mathcal{E}(x)dx \;=\; U(x') - U(x'') + \frac{\mathcal{E}_\circlearrowleft}{N}(x''-x'). \qquad (24)$$

With any function $A(x)$ we can associate a smoothed version using the following definition:

$$\sum_{r=1}^{N} A(x+r)\, e^{U(x+r)-(1/N)\mathcal{E}_\circlearrowleft r} \;\equiv\; A_\varepsilon(x)\, e^{U_\varepsilon(x)}. \qquad (25)$$

In particular the smoothed potential $U_\varepsilon(x)$ is defined by this expression with $A = 1$. Note that without loss of generality it is convenient to have in mind $\mathcal{E}_\circlearrowleft > 0$. (One can always flip the x direction.) Note also that the smoothing scale $N/\mathcal{E}_\circlearrowleft$ becomes larger for smaller SMF. With the above definitions we can write the NESS expression as follows:

$$p_n \;\propto\; \left(\frac{1}{w(x_n)}\right)_\varepsilon e^{-[U(n)-U_\varepsilon(n)]}. \qquad (26)$$

This expression is physically illuminating (see Fig. 3). In the limit of zero SMF it coincides, as expected, with the canonical (Boltzmann) result. For finite SMF the smoothed prefactor and the smoothed potential are not merely constants. Accordingly the preexponential factor becomes important and the "slow" modulation by the Boltzmann factor is flattened. If we take the formal limit of infinite SMF the Boltzmann factor disappears and we are left with $p_n \propto 1/w_n$ as expected from the continuity equation for a resistor network.

VI. STATISTICS OF THE CURRENT

From the preceding analysis it should become clear that the formula for the current can be written schematically as

$$I(\nu) \sim \frac{1}{N}\, w_\varepsilon\, e^{-B} 2\sinh\left(\frac{\mathcal{E}_\circlearrowleft}{2}\right). \qquad (27)$$

In the absence of a potential landscape $[U(x) = 0]$ the formula becomes equivalent to Ohm law: It is a trivial exercise to derive it if all anticlockwise and clockwise rates are equal to the same values $\overrightarrow{w}$ and $\overleftarrow{w}$, respectively, hence $w_\varepsilon = (\overrightarrow{w}\,\overleftarrow{w})^{1/2}$, and $\mathcal{E}_\circlearrowleft = N\ln(\overrightarrow{w}/\overleftarrow{w})$. In the presence of a potential landscape we have an activation barrier. Assuming that the current is dominated by the highest peak a reasonable estimate would be

$$B = \max\{U(x) - U_\varepsilon(x)\} \qquad (28)$$

$$\approx \tfrac{1}{2}[\max\{U\} - \min\{U\}]. \qquad (29)$$

The implication of Eq. (27) with Eq. (28) for the *statistics* of the current is as follows: In the Sinai regime we expect that it will reflect the *log-wide* distribution of the activation factor, while outside of the Sinai regime we expect it to reflect the *normal* distributions of the total resistance w_ε^{-1}, and of the SMF.

In the following sections we provide a detailed analysis for the statistics of $I(\nu)$. We shall see that contrary to first impression the extraction of the fingerprints of the log-normal statistics in the Sinai regime requires extra treatment. The bare statistics is in fact normal in all regimes.

VII. STATISTICS OF CURRENT OUTSIDE OF THE SINAI REGIME

As the driving intensity is increased one observes a crossover from a linear regime, to a Sinai regime, and finally a saturation regime:

$$\text{Linear regime: } \nu < g_{\max}^{-1}, \qquad (30)$$

$$\text{Sinai regime: } g_{\max}^{-1} < \nu < g_{\min}^{-1}, \qquad (31)$$

$$\text{Saturation regime: } \nu > g_{\min}^{-1}. \qquad (32)$$

Consequently we get for the SMF the following approximations:

$$\mathcal{E}_\circlearrowleft \approx \frac{1}{T_B}\begin{cases}\Delta^{(0)}\nu, & \text{linear regime}\\ -\Delta^{(\infty)}/\nu, & \text{saturation regime,}\end{cases} \qquad (33)$$

where

$$\Delta^{(0)} \equiv \sum_n g_{\bar{n}}\Delta_n \sim \pm[2N\,\mathrm{Var}(g)]^{1/2}\Delta, \qquad (34)$$

$$\Delta^{(\infty)} \equiv \sum_n \frac{1}{g_{\bar{n}}}\Delta_n \sim \pm[2N\,\mathrm{Var}(g^{-1})]^{1/2}\Delta. \qquad (35)$$

The estimates for $\Delta^{(0)}$ and for $\Delta^{(\infty)}$ follow from the observation that we have sums of independent random variables. For example $\Delta^{(0)}$ can be rearranged as $\sum_{n=1}^{N}(g_{\bar{n}+1} - g_{\bar{n}})E_n$. Furthermore, we conclude that both $\Delta^{(0)}$ and $\Delta^{(\infty)}$ have normal statistics as implied by the central limit theorem. Consequently we expect normal statistics for the SMF, and hence for the current, as verified in Fig. 4.

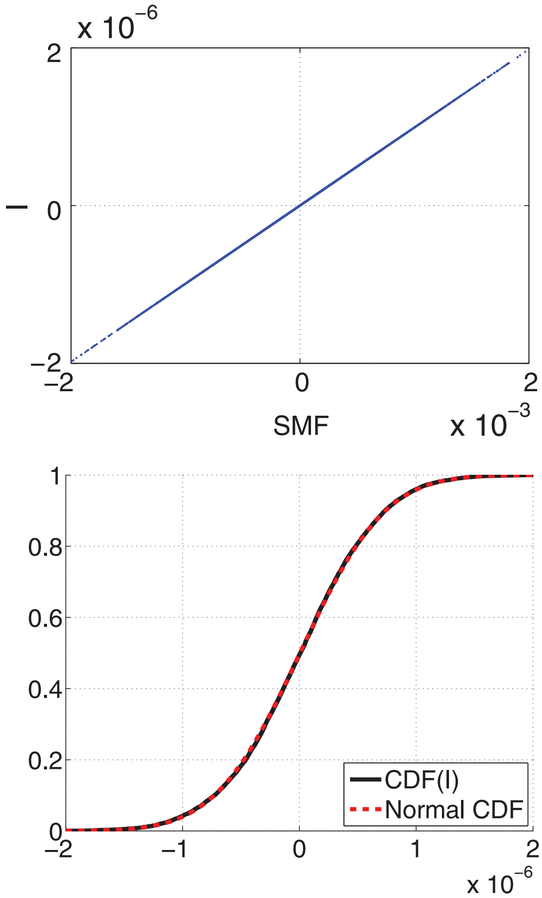

FIG. 4. (Color online) In the linear regime, the current is strongly correlated with the SMF (upper panel), and consequently it has *normal* statistics (lower panel). For the statistical analysis we have generated 10^5 realizations of the ring with $\sigma = 6$.

VIII. STATISTICS IN THE SINAI REGIME

We now focus on the statistics in the Sinai regime. In order to unfold the log-wide statistics it is not a correct procedure to plot blindly the distribution of $\ln(|I|)$. Rather one should look on the joint distribution $(\mathcal{E}_{\circlearrowleft}, I)$ [see Fig. 5(a)]. The nontrivial statistics is clearly apparent. In order to describe it analytically we use the single-barrier estimate of Eq. (28), which is tested in Fig. 5(b). We see that it overestimates the current for small B values (flat landscape) as expected, but it can be trusted for large B where the Sinai physics becomes relevant.

In Fig. 6 we confirm that the probability distribution of the current $P(I;\mathrm{SMF})$, for a given SMF, is the same as the barrier $\exp(-B)$ statistics. We therefore turn to find an explicit expression for the latter.

The probability to have a random-$a$walk trajectory $X_n = U(x_n)$ within $[X_a, X_b]$ equals the survival probability in a diffusion process that starts as a delta function at $X = 0$ with absorbing boundary conditions at X_a and X_b. Integrating over all possible positions of the walls such that $X_b - X_a = R$ is like starting with a uniform distribution between the walls. From here it is straightforward to deduce what is the probability distribution function $f(R)$. The result is displayed in Fig. 7. For the derivation of the exact expression see Appendix A. We note that the occupation-range statistics $f(R)$ is very different from that of maximal-distance statistics $f(K)$ (see Appendix B).

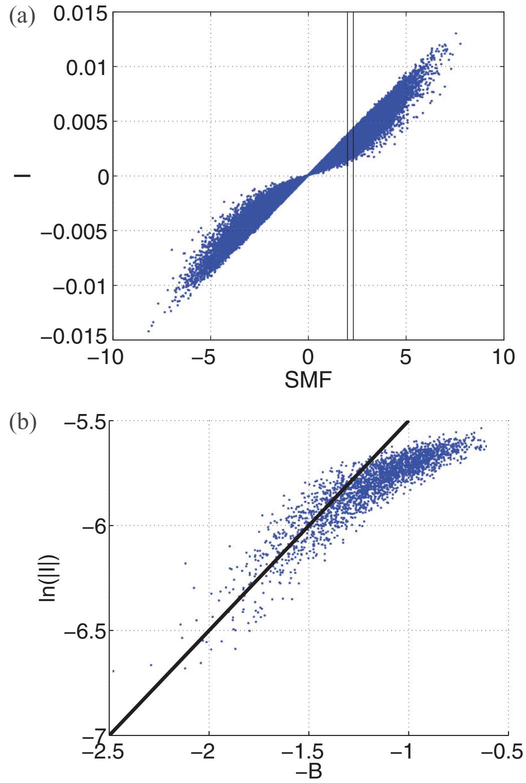

FIG. 5. (Color online) (a) Scatter diagram of the current versus the SMF in the Sinai regime. Note that in the linear regime (see Fig. 4) it looks like a perfect linear correlation with *negligible* transverse dispersion. (b) The correlation between the current I and the barrier B, within the slice $\mathcal{E}_{\circlearrowleft} \in [2.0, 2.1]$. One deduces that the single-barrier approximation is valid for small currents.

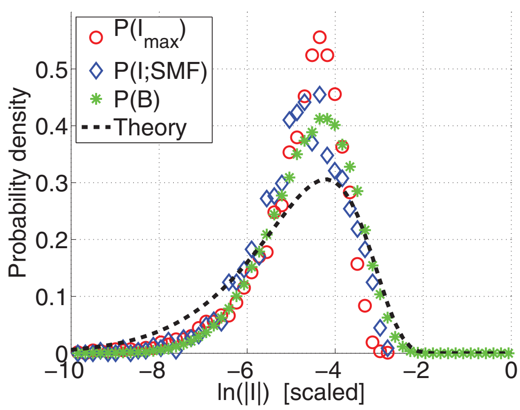

FIG. 6. (Color online) The log-wide distribution $P(I)$ of the current in the Sinai regime is revealed provided a proper procedure is adopted. For theoretical analysis it is convenient to plot a histogram of the I values for a given SMF: The blue diamonds refer to the data of Fig. 5(b). In an actual experiment it is desired to extract statistics from $I(\nu)$ measurements without referring to the SMF: The red empty circles show the statistics of the first maximum of $I(\nu)$. Both distributions look the same, and reflect the barrier statistics (full green circles). The line is the exact version of Eq. (37).

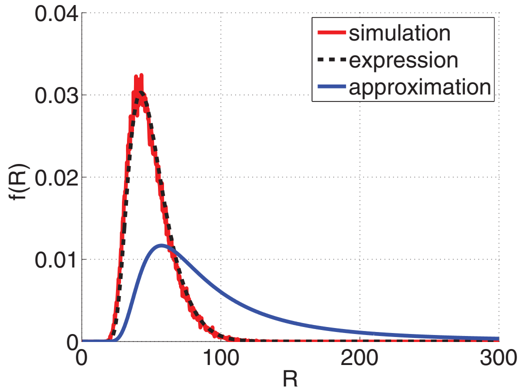

FIG. 7. (Color online) Plot of $f(R)$. Red line is the outcome of a random-walk simulation with $t = 1000$ steps that are Gaussian distributed with unit dispersion. The black dashed line is the exact result, Eq. (A11), while the blue solid line is from the simple asymptotic approximation, Eq. (A13).

Turning back to the problem under consideration, Eq. (29) implies that the probability to have a barrier B is the same as the probability that $U(x)$ occupies a range $R = 2B$. Hence it is described by the probability distribution function $f(R)$ of Fig. 7. The derivation in Appendix A leads to the following practical expression:

$$\text{Prob}\{\text{barrier} < B\} \sim \exp\left[-\frac{1}{2}\left(\frac{\pi\sigma_U}{2B}\right)^2\right], \tag{36}$$

where the variance $\sigma_U^2 = 2DN$ is determined by the diffusion coefficient $D \propto \Delta^2$ that characterizes the potential landscape (see, for example, the illustration in Fig. 3). Taking into account that for a given ν a fraction of the elements in Eq. (11) are effectively zero we get

$$\sigma_U^2 = 2\Delta^2 N\,\frac{\ln(g_{\max}\nu)}{\sigma}. \tag{37}$$

The validity of the exact version of Eq. (36), which is based on Eq. (A11) of Appendix A, has been verified in Fig. 5. No fitting parameters are required.

In an actual experiment it would be desired to extract the statistics from the $I(\nu)$ measurements without referring to the SMF. In Fig. 6 we show that the statistics of the first maximum of $I(\nu)$ is practically the same as $P(I;\text{SMF})$. This means that a simple statistical analysis of "current versus irradiation" curves is enough in order to reveal the fingerprints of Sinai-type physics.

IX. SUMMARY

We have introduced a generalized "random-resistor-network" approach for the purpose of obtaining the NESS current due to nonsymmetric transition rates. Specifically our interest was focused on the NESS of a "glassy" mesoscopic system. The NESS expression clearly interpolates the canonical (Boltzmann) result that applies in equilibrium, with the resistor-network result, that applies at infinite temperature. Due to the "glassiness" the current has novel dependence on the driving intensity, and it possesses unique statistical properties that reflect the Brownian landscape of the stochastic potential. This statistics is related to Sinai's random walk problem, and would not arise if the couplings to the driving source were merely disordered.

From the point of view of a practical experiment, we have assumed that the most accessible measurements would be "current vs irradiation" curves $[I(\nu)]$. Namely, experiments in which one changes the external driving intensity and observes changes in the resulting NESS. The Sinai regime manifests in sign reversals of the current, whose number is estimated in Sec. III.

By repeating such experiments with an ensemble of macroscopically equivalent rings one may find imprints of the Sinai regime in the statistics of the NESS current. Our results, depicted in Fig. 6, suggest that from $I(\nu)$ measurements alone one can extract valuable information regarding the Brownian landscape of the stochastic potential. The functional shape of the distribution provides an indication for having Sinai-type physics, while from its width one can extract the characteristic parameters of the disorder.

ACKNOWLEDGMENTS

This research was supported by the Israel Science Foundation (Grant No. 29/11). We thank Oleg Krichevsky (BGU) for useful advice. S.R. is grateful for support from the Israel Science Foundation (Grant No. 924/11).

APPENDIX A: RANDOM-WALK OCCUPATION-RANGE STATISTICS

In this section we derived the probability density function $f(R)$ to have a random-walk process $x(\cdot)$ of t steps that occupies a range R. This is determined by the probability

$$P_t(x_a,x_b) \equiv \text{Prob}(x_a < x(t') < x_b \text{ for any } t' \in [0,t]). \tag{A1}$$

Accordingly the joint probability density that a random walker would occupy an interval $[x_a,x_b]$ is

$$f(x_a,x_b) = -\frac{d}{dx_a}\frac{d}{dx_b}P_t(x_a,x_b). \tag{A2}$$

It is convenient to use the coordinates

$$X = \frac{x_a + x_b}{2}, \tag{A3}$$

$$R = x_b - x_a. \tag{A4}$$

Consequently the expression for $f(R)$ is

$$f(R) = \int_{-\infty}^{0}\int_{0}^{\infty} dx_a\,dx_b\, f(x_a,x_b)\delta[R-(x_b-x_a)], \tag{A5}$$

$$f(R) = -\int_{-R/2}^{R/2}\left(\frac{1}{4}\partial_X^2 - \partial_R^2\right)P_t(R,X)dX. \tag{A6}$$

Taking into account that $P_t(R,X)$ and its derivatives vanish at the end points $X = \pm(R/2)$ we get

$$f(R) = \int_{-R/2}^{R/2}\partial_R^2 P_t(R,X)dX = \partial_R^2[RP_t(R)], \tag{A7}$$

where $P_t(R)$ is the survival probability of a diffusion process that starts with an initial *uniform* distribution, instead of a random walk that starts as a delta distribution. Optionally we can write

$$\text{Prob}(\text{range} < R) = \partial_R[R P_t(R)]. \tag{A8}$$

We now turn to find an explicit expression for $P_t(R)$. This is done by solving the diffusion equation. Using Fourier expansion the solution is

$$\rho_t(x) = \sum_{n=1,3,5,\ldots}^{\infty} \exp\left[-D\left(\frac{\pi n}{R}\right)^2 t\right] \frac{4}{\pi n R} \sin\left(\frac{\pi n}{R} x\right). \tag{A9}$$

For simplicity we have shifted above the domain to $x \in [0,R]$. For the survival probability we get

$$\begin{aligned} P_t(R) &= \int_0^R \rho_t(x)dx \\ &= \sum_{n=1,3,5,\ldots}^{\infty} \frac{8}{\pi^2 n^2} \exp\left[-D\left(\frac{\pi n}{R}\right)^2 t\right]. \end{aligned} \tag{A10}$$

Using Eq. (A10) in Eq. (A7) we get

$$f(R) = \frac{8\sigma^2}{R^3} \sum_{n=1,3,5,\ldots}^{\infty} \left[\left(\frac{\pi\sigma n}{R}\right)^2 - 1\right] \exp\left[-\frac{1}{2}\left(\frac{\pi\sigma n}{R}\right)^2\right]. \tag{A11}$$

This result is in perfect agreement with the numerical simulation of Fig. 7. Still we would like to have a more compact expression. One possibility is to keep only the first term. The other possibility is to approximate the summation by an integral:

$$\begin{aligned} \text{Prob}(\text{range} < R) &\approx \frac{2}{\pi^2} \frac{\partial}{\partial R}\left[R \int_1^{\infty} \frac{dx}{x^2} \exp\left(-\frac{\pi^2 D t}{R^2} x^2\right)\right] \\ &= \exp\left(-\frac{\pi^2 D t}{R^2}\right). \end{aligned} \tag{A12}$$

Either way we get

$$\text{Prob}(\text{range} < R) \sim \exp\left[-\frac{1}{2}\left(\frac{\pi\sigma}{R}\right)^2\right], \tag{A13}$$

where $\sigma^2 = 2Dt$. This asymptotic expression is illustrated in Fig. 7. Though it does not work very well, it has the obvious advantage of simplicity.

APPENDIX B: RANDOM-WALK MAXIMAL-DISTANCE STATISTICS

The occupation-range statistics of the previous section should not be confused with the maximal-distance statistics. The maximal distance from the initial point is defined as follows:

$$K = \max[x(t)], \quad \text{where} \quad 0 < t < N. \tag{B1}$$

Naively, one might think that the probability distribution of K is similar to the probability distribution of R that has been discussed in the previous section. But this is not true. Furthermore, it is also very sensitive to whether the random walk is constrained to end up at the origin, $x(N) = x(0) = 0$. Without the latter constraint $f(K)$ is finite for small K, but if the constraint is taken into account, it vanishes linearly in this limit.

It is the constrained random-walk process that describes the potential $U(x)$. The exact result for the the K statistics in this case is known [39]:

$$\text{Prob}(K \geqslant k; N) = \frac{\binom{2N}{N-k}}{\binom{2N}{N}}, \quad k = 0,1,2\cdots N. \tag{B2}$$

Switching variables to $\kappa = k/N$ and taking the large N limit, one obtains the probability density function

$$f(\kappa) = N\left[\frac{(1-\kappa)^{\kappa-1}}{(1+\kappa)^{\kappa+1}}\right]^N \ln\left[\frac{1+\kappa}{1-\kappa}\right], \tag{B3}$$

which has a peak at $\kappa \sim 1/\sqrt{2N}$. For $\kappa \ll 1$ this expression can be approximated by the simple function. Switching back

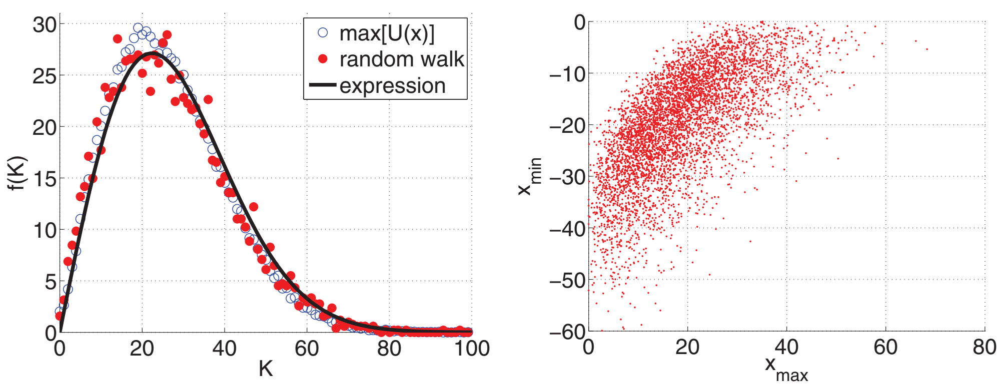

FIG. 8. (Color online) Left panel: Plot of $f(K)$. The histogram of $\max[U(x)]$ values over many ring realizations (blue circles) is compared with the K statistics in a constrained random walk process (red points). The analytical result Eq. (B4) is represented by a black line. Right panel: Scatter plot of $(x_{\min}, x_{\max})$ for the same random walk simulation illustrating the strong correlation.

to K it takes the form

$$f(K) \approx \frac{2K}{N} \exp\left[-\frac{K^2}{N}\right]. \tag{B4}$$

In Fig. 8(a) we illustrate this distribution and demonstrate its applicability to the $U(x)$ of the ring model. In Fig. 8(b) we illustrate the joint distribution of the extreme values $x_{\min} = \min[x(\cdot)]$ and $x_{\max} = \max[x(\cdot)]$. The $f(R)$ distribution of the previous section corresponds to its projection along the diagonal direction, while the $f(K)$ distribution of the present section is its projection along the horizontal or vertical directions.

[1] B. Derrida and Y. Pomeau, Phys. Rev. Lett. **48**, 627 (1982).
[2] S. H. Noskowicz and I. Goldhirsch, Phys. Rev. Lett. **61**, 500 (1988); Phys. Rev. A **42**, 2047 (1990).
[3] J. P. Bouchaud, A. Comtet, A. Georges, and P. Le Doussal, Ann. Phys. (N.Y.) **201**, 285 (1990).
[4] H. E. Roman, M. Schwartz, A. Bunde, and S. Havlin, Europhys. Lett. **7**, 389 (1988).
[5] S. F. Burlatsky, G. S. Oshanin, A. V. Mogutov, and M. Moreau, Phys. Rev. A **45**, R6955 (1992).
[6] Ya. G. Sinai, Theory Probab. Its Appl. **27**, 247 (1982).
[7] S. F. Burlatsky, G. S. Oshanin, A. V. Mogutov, and M. Moreau, Phys. Rev. A **45**, R6955 (1992).
[8] R. L. Schwoebel and E. J. Shipsey, J. Appl. Phys. **37**, 3682 (1966).
[9] M. O. Magnasco, Phys. Rev. Lett. **71**, 1477 (1993).
[10] R. D. Astumian and M. Bier, Phys. Rev. Lett. **72**, 1766 (1994).
[11] M. O. Magnasco, Phys. Rev. Lett. **72**, 2656 (1994).
[12] P. Reimann, Phys. Rep. **361**, 57 (2002).
[13] C. T. MacDonald, J. H. Gibbs, and A. C. Pipkin, Biopolymers **6**, 1 (1968).
[14] H. X. Zhou and Y. D. Chen, Phys. Rev. Lett. **77**, 194 (1996).
[15] E. Frey and K. Kroy, Ann. Phys. **14**, 20 (2005).
[16] A. B. Kolomeisky and M. E. Fisher, Annu. Rev. Phys. Chem. **58**, 675 (2007).
[17] B. Xu, P. Zhang, X. Li, and N. Tao, Nano Lett. **4**, 1105 (2004).
[18] H. W. Fink and C. Schönenberger, Nature (London) **398**, 407 (1999).
[19] K. W. Kehr, K. Mussawisade, T. Wichmann, and W. Dieterich, Phys. Rev. E **56**, R2351 (1997).
[20] A. Heuer, S. Murugavel, and B. Roling, Phys. Rev. B **72**, 174304 (2005).
[21] S. Murugavel and B. Roling, J. Non-Cryst. Solids **351**, 2819 (2005).
[22] B. Roling, S. Murugavel, A. Heuer, L. Luhning, R. Friedrich, and S. Rothel, Phys. Chem. Chem. Phys. **10**, 4211 (2008).
[23] M. Einax, M. Korner, P. Maass, and A. Nitzan, Phys. Chem. Chem. Phys. **12**, 645 (2010).
[24] F. Ritort and P. Sollich, Adv. Phys. **52**, 219 (2003).
[25] A. Crisanti and F. Ritort, J. Phys. A **36**, R181 (2003).
[26] D. Cohen, Phys. Scr., T **151**, 014035 (2012), and further references therein.
[27] M. Sales, J.-P. Bouchaud, and F. Ritort, J. Phys. A **36**, 665 (2003).
[28] D. K. Lubensky and D. R. Nelson, Phys. Rev. E **65**, 031917 (2002).
[29] F. Corberi, A. de Candia, E. Lippiello, and M. Zannetti, Phys. Rev. E **65**, 046114 (2002).
[30] S. Luding, M. Nicolas, and O. Pouliquen, in *Compaction of Soils, Granulates and Powders*, edited by D. Kolymbas and W. Fellin (Balkema, Rotterdam, 2000), p. 241.
[31] D. Hurowitz and D. Cohen, Europhys. Lett. **93**, 60002 (2011).
[32] D. Hurowitz, S. Rahav, and D. Cohen, Europhys. Lett. **98**, 20002 (2012).
[33] J. L. Lebowitz and H. Spohn, J. Stat. Mech.: Theory Exp.**95**, 333 (1999).
[34] P. Gaspard, J. Chem. Phys. **120**, 8898 (2004).
[35] Udo Seifert, Phys. Rev. Lett. **95**, 040602 (2005).
[36] D. Andrieux and P. Gaspard, J. Stat. Phys. **127**, 107 (2007).
[37] Adrienne W. Kemp, Adv. Appl. Probab. **19**, 505 (1987).
[38] W. Feller, *An Introduction to Probability Theory and its Applications* (Wiley, New York, 1950).
[39] Meyer Dwass, Ann. Math. Stat. **38**, 1042 (1967).
[40] J. Schnakenberg, Rev. Mod. Phys. **48**, 571 (1976).
[41] T. L. Hill, J. Theor. Biol. **10**, 442 (1966).
[42] R. K. P. Zia and B. Schmittmann, J. Stat. Mech. (2007), P07012.